Anesthesiology
83:361–373, 1995

Differential Effects of Isoflurane and Halothane on Aortic Input Impedance Quantified Using a Three-element Windkessel Model

Douglas A. Hettrick, Ph.D., Paul S. Pagel, M.D., Ph.D.,† David C. Warltier, M.D., Ph.D.‡*

Background: **Systemic vascular resistance (the ratio of mean aortic pressure [AP] and mean aortic blood flow [AQ]) does not completely describe left ventricular (LV) afterload because of the phasic nature of pressure and blood flow. Aortic input impedance (Z_{in}) is an established experimental description of LV afterload that incorporates the frequency-dependent characteristics and viscoelastic properties of the arterial system. Z_{in} is most often interpreted through an analytical model known as the three-element Windkessel. This investigation examined the effects of isoflurane, halothane, and sodium nitroprusside (SNP) on Z_{in}. Changes in Z_{in} were quantified using three variables derived from the Windkessel: characteristic aortic impedance (Z_c), total arterial compliance (C), and total arterial resistance (R).**

Methods: **Sixteen experiments were conducted in eight dogs chronically instrumented for measurement of AP, LV pressure, maximum rate of change in left ventricular pressure, subendocardial segment length, and AQ. AP and AQ waveforms were recorded in the conscious state and after 30 min equilibration at 1.25, 1.5, and 1.75 minimum alveolar concentration (MAC) isoflurane and halothane. Z_{in} spectra were obtained by power spectral analysis of AP and AQ waveforms and corrected for the phase responses of the transducers. Z_c and R were calculated as the mean of Z_{in} between 2 and 15 Hz and the difference between Z_{in} at zero frequency and Z_c, respectively. C was determined using the formula $C = (A_d \cdot MAP) \cdot [MAQ \cdot (P_{es} - P_{ed})]^{-1}$, where A_d = diastolic AP area; MAP and MAQ = mean AP and mean AQ, respectively; and P_{es} and P_{ed} = end-systolic and end-diastolic AP, respectively. Parameters describing the net site and magnitude of arterial wave reflection were also calculated from Z_{in}. Eight additional dogs were studied in the conscious state before and after 15 min equilibration at three equihypotensive infusions of SNP.**

Results: **Isoflurane decreased R (3,205 ± 315 during control to 2,340 ± 2.19 $dyn \cdot s \cdot cm^{-5}$ during 1.75 MAC) and increased C (0.55 ± 0.02 during control to 0.73 ± 0.06 $ml \cdot mmHg^{-1}$ during 1.75 MAC) in a dose-related manner. Isoflurane also increased Z_c at the highest dose. Halothane increased C and Z_c but did not change R. Equihypotensive doses of SNP decreased R and produced marked increases in C without changing Z_c. No changes in the net site or the magnitude of arterial wave reflection were observed with isoflurane and halothane, in contrast to the findings with SNP.**

Conclusions: **The major difference between the effects of isoflurane and halothane on LV afterload derived from the Windkessel model of Z_{in} was related to R, a property of arteriolar resistance vessels, and not to Z_c or C, the mechanical characteristics of the aorta. No changes in arterial wave reflection patterns determined from Z_{in} spectra occurred with isoflurane and halothane. These results indicate that isoflurane and halothane have no effect on frequency-dependent arterial properties. (Key words: Anesthetics, volatile: halothane; isoflurane. Heart: left ventricular afterload. Hemodynamics: aortic blood flow; aortic pressure. Signal processing: coherence function; power spectrum analysis. Vasodilators: sodium nitroprusside.)**

ALTHOUGH a definition of afterload that describes the mechanical properties of the arterial vasculature opposing left ventricular ejection is intuitively clear,[1] quantitative evaluation of afterload *in vivo* remains difficult. Systemic vascular resistance, calculated as the ratio of mean arterial pressure and mean arterial blood flow, is the most commonly used estimate of left ventricular afterload, but this parameter alone can not completely describe afterload because of the dynamic, phasic nature of the arterial pressure and blood flow waveforms. Aortic input impedance (Z_{in}) is the complex ratio of aortic pressure and aortic blood flow containing real and imaginary mathematical elements expressed in terms of modulus and phase angle spectra in the frequency (ω) domain.[2–4] $Z_{in}(\omega)$ incorporates the viscoelastic and resistive properties of the arterial

* Biomedical Engineer, Department of Anesthesiology.

† Assistant Professor, Department of Anesthesiology.

‡ Professor, Departments of Anesthesiology, Pharmacology, and Medicine (Division of Cardiology); Vice Chair for Research, Department of Anesthesiology.

Received from the Departments of Anesthesiology, Pharmacology, and Medicine, Medical College of Wisconsin, and the Zablocki Department of Veterans Affairs Medical Center, Milwaukee, Wisconsin. Submitted for publication December 28, 1994. Accepted for publication April 10, 1995. Supported by United States Public Health Service grant HL 32911, Anesthesiology Research Training Grant GM 08377, and Department of Veterans Affairs Medical Research Funds.

Address reprint requests to Dr. Warltier: Department of Anesthesiology, MEB, Room 462C, Medical College of Wisconsin, 8701 Watertown Plank Road, Milwaukee, Wisconsin 53226.

system and has become a widely accepted experimental description left ventricular afterload.[1] However, many of the features of the aortic input impedance spectrum are difficult to quantify because of frequency dependence. As a result, $Z_{in}(\omega)$ is often interpreted through an analytical model known as the three-element Windkessel.[4]

An electrical representation of time-dependent arterial blood flow through the Windkessel consists of a resistor (characteristic aortic impedance [Z_c]) in series with a parallel combination of a second resistor (total arterial resistance [R]) and a capacitor (total arterial compliance [C]) (fig. 1).[5,6] Z_c is determined by the Poiseullian resistance of the aorta and the compliance of this vessel. Characteristic aortic impedance is represented as a resistor in the model for simplicity and because its value does not vary significantly with frequency.[7,8] R represents the combined Pouiseullian resistances of the entire arterial vascular tree. The sum of R and Z_c is mathematically equivalent to systemic vascular resistance calculated as the ratio of mean arterial pressure to mean aortic blood flow. C is the energy storage element of the Windkessel. These elements of the arterial system interact with the mechanical properties of the left ventricle to determine overall cardiovascular performance. Aortic input impedance can be determined as a function of frequency from these variables using the equation[9]: $Z_{in}(\omega) = Z_c + R \cdot (1 + j \cdot \omega \cdot C \cdot R)^{-1}$, where $j = (-1)^{1/2}$ Investigations have indicated that the three-element Windkessel provides an excellent approximation of aortic input impedance under a wide variety of physiologic conditions,[4,6] allowing quantification of changes in afterload derived from $Z_{in}(\omega)$ to be described using these derived variables.

The effects of volatile anesthetics, including isoflurane and halothane, on quantitative indices of left ventricular afterload have not been described. It has been widely demonstrated that isoflurane, in contrast to halothane, causes dose-related decreases in calculated systemic vascular resistance in dogs[10–15] and humans,[16,17] suggesting that this inhalational agent reduces left ventricular afterload. However, the effects of isoflurane and halothane on specific arterial compliance and resistance variables must be examined to provide a more complete understanding of the actions of these anesthetics on arterial mechanical properties. Therefore, this investigation was undertaken to characterize the effects of isoflurane and halothane on aortic input impedance and to quantify alterations in afterload produced by these agents using the three-element Windkessel model in chronically instrumented dogs. A parallel series of experiments were conducted using equihypotensive infusions of sodium nitroprusside as positive controls.

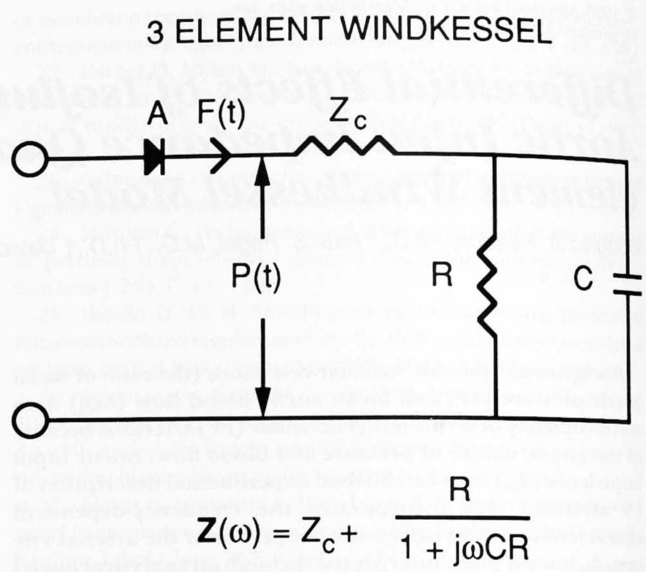

Fig. 1. Electrical analog of the three-element Windkessel model of aortic input impedance ($Z(\omega)$). Diode A represents the aortic valve. Time-dependent blood flow ($F(t)$) entering the arterial system first encounters the resistance of the ascending aorta (characteristic aortic impedance (Z_c)). Further flow is dictated by total arterial resistance (R) and total arterial compliance (C), the energy storage component of the arterial vasculature. $P(t)$ = time-dependent aortic pressure; ω = frequency; $j = \sqrt{-1}$.

Materials and Methods

All experimental procedures and protocols used in this investigation were reviewed and approved by the Animal Care Committee of the Medical College of Wisconsin. All procedures conformed to the American Physiologic Society Guiding Principles in the Care and Use of Animals§ and were performed in accordance with the National Institutes of Health Guide for the Care and Use of Laboratory Animals.‖

§ Guiding Principles in the Care and Use of Animals. Bethesda, The American Physiological Society, revised 1991.

‖ Guide for the Care and Use of Laboratory Animals. Publication NIH 85-23. Bethesda, National Institutes of Health, Department of Health and Human Services, revised 1985.

General Preparation

Surgical implantation of instruments has been previously described in detail.[13,18] In the presence of general anesthesia and using aseptic techniques, conditioned mongrel dogs underwent a left thoracotomy and heparin-filled catheters were placed in the proximal descending thoracic aorta and the right atrium for measurement of aortic pressure and fluid or drug administration, respectively. An ultrasonic transit-time flow probe (Transonic Systems, Ithaca, NY) was positioned around the ascending thoracic aorta for measurement of continuous aortic flow (fig. 2). A pair of miniature ultrasonic segment length transducers (5 MHz) were implanted in the left ventricular subendocardium for measurement of changes in regional contractile function (percentage segment shortening [%SS]). A high-fidelity micromanometer (P7, Konigsberg Instruments, Pasadena, CA) was positioned in the left ventricle for measurement of continuous left ventricular pressure and the maximum rate of increase in left ventricular pressure (dP/dt). A heparin-filled catheter was inserted directly into the left atrial appendage, and the left ventricular micromanometer was cross-calibrated *in vivo* against pressures measured with arterial and left atrial catheters (P_{50} pressure transducer, Gould Instruments, Oxnard, CA). All instrumentation was secured, tunneled between the scapulae, and exteriorized through several small incisions. The pericardium was left widely open, the chest wall closed in layers, and the pneumothorax evacuated by a chest tube. Each dog was fitted with a jacket (Alice King Chatham, Los Angeles, CA) to prevent damage to the instruments and catheters, which were housed in an aluminum box within the jacket pocket.

All dogs received systemic analgesics (fentanyl and droperidol [Innovar-Vet], Pittman-Moore, Mundelein, IL] as needed after surgery. Dogs were allowed to recover a minimum of 7 days before experimentation, during which time all were treated with intramuscular antibiotics [cephalothin ($40\ mg \cdot kg^{-1}$) and gentamicin ($4.5\ mg \cdot kg^{-1}$)] and were trained to stand quietly in an animal sling during recording of hemodynamics. Segment length signals were monitored with an ultrasonic amplifier (Crystal Biotech, Hopkinton, MA). End-systolic and end-diastolic segment lengths were measured at maximum negative left ventricular dP/dt and just before the onset of left ventricular isovolumic contraction, respectively. The lengths were normalized according to the method of Theroux *et al.*[19] %SS was calculated using the equation: $\%SS = (EDL - ESL) \cdot 100 \cdot EDL^{-1}$, where ESL = end-systolic segment length and EDL = end-diastolic segment length. Hemodynamic data were continuously recorded on a polygraph (7758A, Hewlett-Packard, San Francisco, CA) and digitized by a computer interfaced with an analog to digital converter.

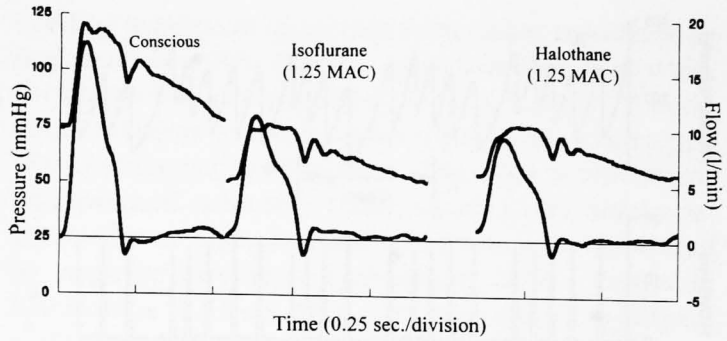

Fig. 2. Aortic pressure and blood flow waveforms in the conscious state and during isoflurane and halothane anesthesia (1.25 MAC) in a typical dog. Alterations in the relation between left ventricular and arterial mechanical properties produce changes in the morphologic characteristics of the waveforms.

Determination of Aortic Input Impedance Spectra

Aortic input impedance spectra were determined from digitized, steady-state aortic blood pressure and aortic blood flow waveforms using the techniques of Taylor[20] and Burkhoff *et al.*[4] Data files consisting of 4,096 points were sampled at 200 Hz (20.48 s; frequency increment = 0.098 Hz) and were divided into five 2,048 point bins with 512 point overlap. A Hamming window was applied to each bin to reduce side lobe leakage. The autopower spectrum of the aortic blood pressure [$P_{pp}(\omega)$], aortic blood flow [$P_{ff}(\omega)$], and cross power spectrum between aortic pressure and blood flow waveforms [$P_{pf}(\omega)$] were determined using a Welch periodogram technique.[21,22] The aortic input impedance [$Z_{in}(\omega)$] was calculated as a function of frequency using the formula $Z_{in}(\omega) = P_{pp}(\omega) \cdot [P_{pf}(\omega)]^{-1}$. Each impedance spectrum was calculated to a maximum frequency of 15 Hz because little spectral energy exists above this frequency in the cardiovascular system.[1] This range of frequency analysis encompassed 6–15 harmonics for the aortic pressure and blood flow waveforms evaluated in all dogs.

The calculated impedance spectra were corrected for the phase response of aortic flow probe and aortic pressure transducer (see appendix). The magnitude of the frequency response of the flow meter was flat from 0 to 15 Hz with the analog low-pass filter cutoff set to

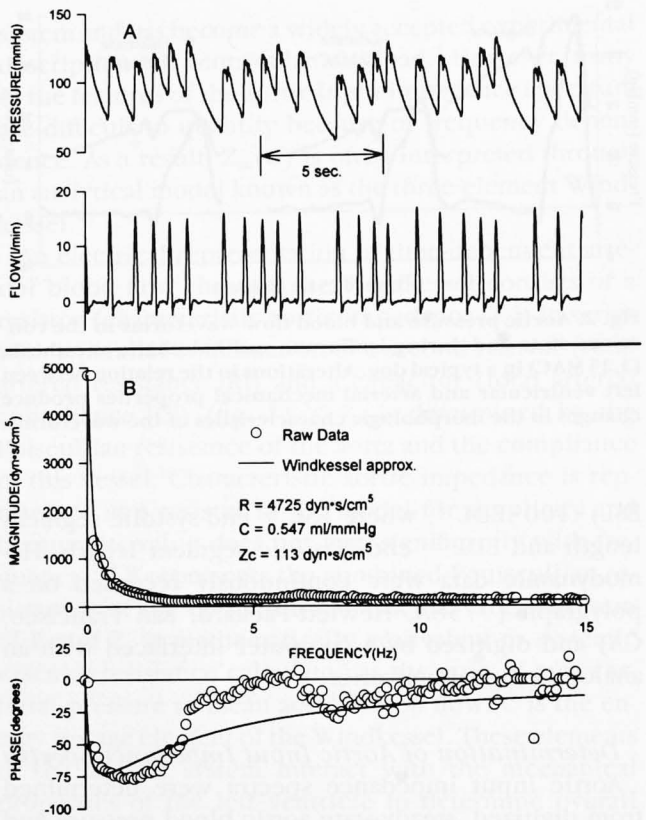

Fig. 3. Calculation of the aortic input impedance spectrum in a typical experiment in a conscious dog. (*A*) Raw aortic pressure and blood flow waveforms consisting of 4,096 data points were sampled at 200 Hz in a conscious dog. (*B*) The corresponding aortic input impedance spectrum (open circles) consisting of magnitude (*top*) and phase (*bottom*) components were calculated by spectral analysis. An completely continuous spectrum was formed in this dog with a prominent sinus arrhythmia because of multiple fundamental frequencies and corresponding harmonics. Frequencies with magnitude squared coherence values less than 0.8 were discarded. R = total arterial resistance; C = total arterial compliance; Z_c = characteristic aortic impedance. Solid lines = the frequency response of best-fit Windkessel parameters.

30 Hz. The phase delay of this signal was 11.2 ms independent of frequency. The frequency response of the fluid-filled pressure transducer catheter system was determined by performing a quick-release, or "pop," test.[1] The undamped natural frequency of this system was found to be 15.1 Hz with a damping ratio of 0.16 (see appendix). Because of the nonlinear phase response of the pressure transducer system, the time delay of the aortic blood pressure waveform was frequency-dependent and was corrected in the frequency domain using the method of Milnor.[1] Additional error in the phase of the pressure signal because of the distance (approximately 4 cm) between the flow probe (ascending thoracic aorta) and the pressure transducer (descending thoracic aorta) was also corrected using standard techniques.[23]

Correlation of aortic pressure and blood flow waves at each frequency of the input impedance spectrum was determined using the magnitude squared coherence: MSC(ω) $|P_{pf}(\omega)|^2 \cdot [P_{pp}(\omega) \cdot P_{ff}(\omega)]^{-1}$, where MSC = magnitude squared coherence. Magnitude squared coherence values vary between 0 (no correlation between pressure and flow) and 1 (matched correlation). Higher correlation between aortic pressure and blood flow waveforms increases the precision of the impedance value at a given frequency. Input impedance data with mean squared coherence values less than 0.8 were discarded. High coherence was observed at most frequencies in conscious dogs as a result of heart rate variability caused by the sinus arrhythmia (fig. 3), a finding that resulted in the elimination of less than 10% of $Z_{in}(\omega)$ data points. Heart rate variability creates a large number of "fundamental" heart rates and corresponding harmonics, resulting in a nearly continuous input impedance spectrum. In contrast, little or no sinus arrhythmia occurred during isoflurane or halothane anesthesia and heart rate remained relatively constant at each anesthetic concentration. Thus, high coherence impedance measurements were grouped around harmonics of this fundamental frequency (*i.e.*, heart rate) during each anesthetic intervention. Under these circumstances, a greater percentage of spectral points in $Z_{in}(\omega)$ between the fundamental frequency and harmonics were eliminated resulting in a less continuous aortic input impedance spectrum (fig. 4).[22]

Z_c was determined from the aortic input impedance spectra as the mean of the magnitude of $Z_{in}(\omega)$ ($|Z_{in}(\omega)|$) between 2 and 15 Hz.[4,24,25] R was calculated as the difference between the value of $|Z_{in}(\omega)|$ at zero frequency and Z_c. $|Z_{in}(\omega)|$ at zero frequency is equal to systemic vascular resistance determined as the ratio of mean arterial pressure and mean aortic blood flow (*i.e.*, cardiac output).[1] The C component of the Windkessel model was calculated using the method of Liu *et al.*[26]:

$$C = (A_d \cdot MAQ) \cdot [MAP \cdot (P_{es} - P_{ed})]^{-1},$$

where A_d = the area under the diastolic portion of the arterial pressure curve above mean venous pressure (assumed to be 0 mmHg); MAP = mean arterial pressure; MAQ = mean aortic blood flow; P_{es} = end-systolic aortic pressure; and P_{ed} = end-diastolic aortic pressure. Because this method does not assume a monoexponen-

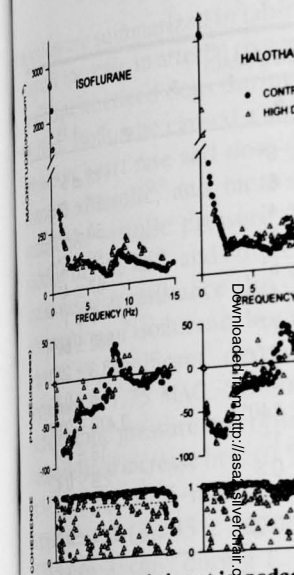

Fig. 4. Typical aortic input impedan
phase (*middle graphs*), and cohere
obtained in the same dog on thre
control state (circles) and with hig
thane, and sodium nitroprusside (
with magnitude squared coherenc
are not included in the top and m

tial decay of the aortic pressur
of C can be performed in th
waves from the distal arterial
C was determined from the av
beats for each intervention. A
distance to the net site of arte
first minimum of $|Z_{in}(\omega)|$ (F_{mi}
intervention. Lastly, the arteri
($\Delta Z/Z_c$), defined as the ratio o
$Z_{in}(\omega)|$ at F_{min} and the follow
and Z_c was also determined.
the magnitude of the reflecte

Experimental Protocols

In two sets of experiments,
± 1 kg, mean ± SEM) were as
rane or halothane in a randor
separate days. Dogs were fas
deficits were replaced before
talloid (500 ml 0.9% saline).
continued at 3 ml · kg^{-1} · h^{-1}
experiment. After instruments
systemic hemodynamics wer
scious state. Continuous aorti
tic blood flow waveforms wer
eration and analysis of $Z_{in}(\omega)$.

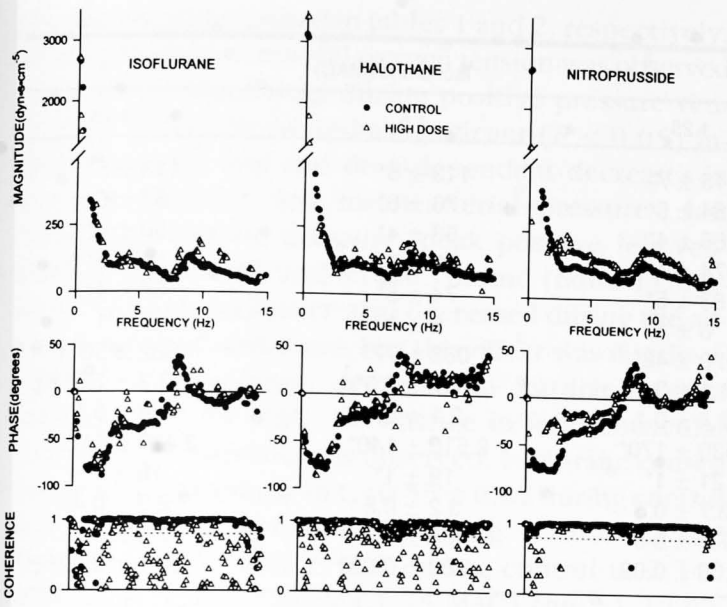

Fig. 4. Typical aortic input impedance magnitude (*top graphs*), phase (*middle graphs*), and coherence (*bottom graphs*) spectra obtained in the same dog on three experimental days in the control state (circles) and with high doses of isoflurane, halothane, and sodium nitroprusside (triangles). Frequency points with magnitude squared coherence less than 0.8 (dashed line) are not included in the top and middle graphs.

tial decay of the aortic pressure waveform, calculation of C can be performed in the presence of reflected waves from the distal arterial vasculature. The value of C was determined from the average of five consecutive beats for each intervention. A variable that predicts the distance to the net site of arterial wave reflections, the first minimum of $|Z_{in}(\omega)|$ (F_{min}) was calculated at each intervention. Lastly, the arterial wave reflection factor ($\Delta Z/Z_c$), defined as the ratio of the difference between $|Z_{in}(\omega)|$ at F_{min} and the following maximum of $|Z_{in}(\omega)|$ and Z_c was also determined. $\Delta Z/Z_c$ is proportional to the magnitude of the reflected waves.

Experimental Protocols

In two sets of experiments, dogs (n = 8; weight 26 ± 1 kg, mean ± SEM) were assigned to receive isoflurane or halothane in a random manner (coin toss) on separate days. Dogs were fasted overnight, and fluid deficits were replaced before experiments with crystalloid (500 ml 0.9% saline). Maintenance fluids were continued at 3 $ml \cdot kg^{-1} \cdot h^{-1}$ for the duration of each experiment. After instruments were calibrated, baseline systemic hemodynamics were recorded in the conscious state. Continuous aortic blood pressure and aortic blood flow waveforms were recorded for later generation and analysis of $Z_{in}(\omega)$. Dogs were then anesthetized by inhalation induction with either halothane or isoflurane in 100% oxygen. After tracheal intubation, anesthesia was maintained at 1.25, 1.5, or 1.75 minimum alveolar concentration (MAC) in a nitrogen (79%)–oxygen (21%) mixture. The order of MAC levels was assigned randomly (Latin square). End-tidal concentration of isoflurane and halothane were measured by mass spectrometry (Advantage 2000, Marquette Electronics, St. Louis, MO). The mass spectrometer was calibrated with known standards before and during experimentation. The canine MAC values for isoflurane and halothane used in this investigation were 1.28% and 0.86%, respectively. Systemic hemodynamics and aortic pressure and blood flow waveforms were recorded after 1 h equilibration at each end-tidal anesthetic concentration. Arterial blood gas tensions were maintained at conscious levels in all anesthetized dogs by adjustment of nitrogen and oxygen concentrations and respiratory rate throughout each experiment.

In a third set of experiments using an additional group of conscious dogs (n = 8; weight = 26 ± 1 kg), continuous intravenous infusions of sodium nitroprusside were administered after baseline systemic hemodynamics and aortic pressure and blood flow waveforms had been recorded. The infusions of sodium nitroprusside (range 0.25–3 $\mu g \cdot kg^{-1} \cdot min^{-1}$) were adjusted to decrease mean arterial pressure approximately 20, 30 and 50%, corresponding to decreases in mean arterial pressure observed during isoflurane and halothane anesthesia at 1.25, 1.5, and 1.75 MAC. After a 15-min equilibration period, cardiovascular parameters and aortic pressure and blood flow waveforms for subsequent $Z_{in}(\omega)$ generation were recorded under steady state conditions at each infusion rate of sodium nitroprusside.

Statistical Analysis

Statistical analysis of data within and between groups in the conscious state during anesthetic interventions and during sodium nitroprusside infusions was performed by multiple analysis of variance with repeated measures followed by applications of the students *t* test with Duncan's correction for multiplicity. Changes within and between groups were considered statistically significant when the *P* value was less than 0.05. All data were expressed as mean ± SEM.

Results

The effects of isoflurane and halothane on systemic hemodynamics and characteristics of arterial wave re-

Table 1. Systemic Hemodynamic Effects of Isoflurane

	N	Conscious Control	Isoflurane (MAC) 1.25	1.5	1.75
HR (beats/min)	8	87 ± 5	115 ± 7*	113 ± 6*	113 ± 5*
SBP (mmHg)	8	111 ± 4	84 ± 5*	76 ± 6*	67 ± 5*†
DBP (mmHg)	8	76 ± 4	65 ± 4*	58 ± 4*	50 ± 4*†
MBP (mmHg)	8	91 ± 4	74 ± 4*	65 ± 5*	56 ± 5*†
LVSP (mmHg)	7	113 ± 4	83 ± 5*	74 ± 5*	67 ± 4*†
LVEDP (mmHg)	7	8 ± 1	6 ± 1	6 ± 1	6 ± 1
dP/dt ($mmHg \cdot s^{-1}$)	7	2,119 ± 145	1,272 ± 48*	1,063 ± 77*	932 ± 50*†
SS (%)	8	25.6 ± 2.6	21.1 ± 3.1*	17.7 ± 3.0*†	13.3 ± 2.5*†‡
CO ($L \cdot min^{-1}$)	8	2.5 ± 0.2	2.4 ± 0.1	2.1 ± 0.1	1.8 ± 0.1*
SVR ($dyne \cdot s \cdot cm^{-5}$)	8	3,110 ± 270	2,530 ± 170*	2,510 ± 140*	2,470 ± 210*
SV (ml)	8	28 ± 2	21 ± 1*	19 ± 1*	16 ± 1*†
F_{min} (Hz)	8	2.8 ± 0.1	3.7 ± 0.3	3.2 ± 0.5	2.9 ± 0.4
$\Delta Z/Z_c$ (10^2)	8	9.0 ± 1.1	7.4 ± 0.8	6.8 ± 1.4	7.0 ± 1.8
ET (%)	8	—	1.58 ± 0.02	1.88 ± 0.02†	2.21 ± 0.02†‡

Data are mean ± SEM.

HR = heart rate; SBP, DBP, and MBP = systolic, diastolic, and mean aortic blood pressure, respectively; LVSP and LVEDP = left ventricular systolic and end-diastolic pressure, respectively; SS = segment shortening; CO = cardiac output; SV = stroke volume; SVR = systemic vascular resistance; F_{min} = frequency at first impedance modulus minimum; $\Delta Z/Z_c$ = arterial wave reflection index; ET = end-tidal isoflurane concentration.

* Significantly ($P < 0.05$) different from conscious control.

† Significantly ($P < 0.05$) different from 1.25 MAC isoflurane.

‡ Significantly ($P < 0.05$) different from 1.5 MAC isoflurane.

Table 2. Systemic Hemodynamic Effects of Halothane

	N	Conscious Control	Halothane (MAC) 1.25	1.5	1.75
HR (beats/min)	8	85 ± 7	95 ± 5	101 ± 5*	109 ± 6*†
SBP (mmHg)	8	117 ± 4	87 ± 3*	80 ± 4*	72 ± 5*†
DBP (mmHg)	8	81 ± 4	69 ± 3*	62 ± 3*	57 ± 5*†
MBP (mmHg)	8	92 ± 3	76 ± 3*	69 ± 3*	62 ± 4*†
LVSP (mmHg)	7	120 ± 4	86 ± 3*	81 ± 4*	73 ± 5*†
LVEDP (mmHg)	7	7 ± 0	8 ± 2	8 ± 2	8 ± 1
dP/dt ($mmHg \cdot s^{-1}$)	7	2,216 ± 113	1,105 ± 48*	997 ± 36*	872 ± 46*†
SS (%)	8	25.4 ± 2.6	18.7 ± 2.2*	15.2 ± 1.7*†	12.3 ± 1.1*†‡
CO ($L \cdot min^{-1}$)	8	2.3 ± 0.2	1.8 ± 0.1*	1.7 ± 0.1*	1.6 ± 0.1*
SVR ($dyne \cdot s \cdot cm^{-5}$)	8	3,460 ± 270	3,350 ± 190	3,290 ± 250	3,240 ± 260
SV (ml)	8	27 ± 3	20 ± 1*	17 ± 1*	15 ± 1*†
F_{min} (Hz)	8	2.6 ± 0.1	2.8 ± 0.4	2.3 ± 0.3	2.1 ± 0.2
$\Delta Z/Z_c$ (10^2)	8	8.4 ± 0.8	6.6 ± 1.0	9.6 ± 0.8	7.5 ± 0.8
ET (%)	8	—	1.08 ± 0.02	1.31 ± 0.01†	1.54 ± 0.02†‡

Data are mean ± SEM.

HR = heart rate; SBP, DBP, and MBP = systolic, diastolic, and mean aortic blood pressure, respectively; LVSP and LVEDP = left ventricular systolic and end-diastolic pressure, respectively; SS = segment shortening; CO = cardiac output; SV = stroke volume; SVR = systemic vascular resistance; F_{min} = frequency at first impedance modulus minimum; $\Delta Z/Z_c$ = arterial wave reflection index; ET = end-tidal halothane concentration.

* Significantly ($P < 0.05$) different from conscious control.

† Significantly ($P < 0.05$) different from 1.25 MAC halothane.

‡ Significantly ($P < 0.05$) different from 1.5 MAC halothane.

flection are summarized in tables 1 and 2, respectively. A small increase in arterial oxygen tension was observed in all anesthetized dogs during positive pressure ventilation. Isoflurane caused a significant ($P < 0.05$) increase in heart rate and dose-dependent decreases in systolic, diastolic, and mean arterial pressures, left ventricular systolic pressure, peak positive left ventricular dP/dt, %SS, and stroke volume (table 1). Systemic vascular resistance also decreased during the administration of isoflurane, but this effect was not dose-related. A significant decrease in cardiac output occurred at 1.75 MAC. No change in left ventricular end-diastolic pressure was observed. Isoflurane caused a dose-related increase in C (0.55 ± 0.02 during control to 0.73 ± 0.06 ml · mmHg^{-1} during 1.75 MAC) and decrease in R (3,205 ± 315 during control to 2,340 ± 219 dyn · s · cm^{-5} during 1.75 MAC) (fig. 5). Isoflurane also increased Z_c at the highest dose. No changes in F_{min} or $\Delta Z/Z_c$ occurred during administration of isoflurane (table 1), indicating that the distal site of net arterial wave reflection and the magnitude of the reflected waves were unaffected by this volatile anesthetic.

Halothane anesthesia produced hemodynamic alterations that were similar to those observed with isoflurane. Dose-related increases in heart rate and decreases in arterial pressures, left ventricular systolic pressure, dP/dt, %SS, and stroke volume occurred during administration of halothane (table 2). In contrast to the findings with isoflurane, however, halothane caused dose-related decreases in cardiac output concomitant with maintenance of systemic vascular resistance at levels present in the conscious state. Halothane increased C (0.56 ± 0.02 during control to 0.65 ± 0.05 ml · mmHg^{-1} during 1.75 MAC), however, increases in C were not dose-related (fig. 5). No changes in R were observed during administration of halothane, in contrast to the observations during isoflurane anesthesia. Halothane also increased Z_c at 1.75 MAC. No changes in F_{min} and $\Delta Z/Z_c$ occurred with halothane, indicating that this anesthetic did not alter the pattern or magnitude of arterial wave reflections (table 2).

Sodium nitroprusside caused dose-related increases in heart rate and decreases in systolic, diastolic, and mean arterial pressures, left ventricular systolic and end-diastolic pressures, and systemic vascular resistance (table 3). No changes in dP/dt, %SS, or cardiac output occurred. Sodium nitroprusside caused dose-dependent increases in C (0.51 ± 0.02 during control to 1.36 ± 0.16 ml · mmHg^{-1} during the high dose) and

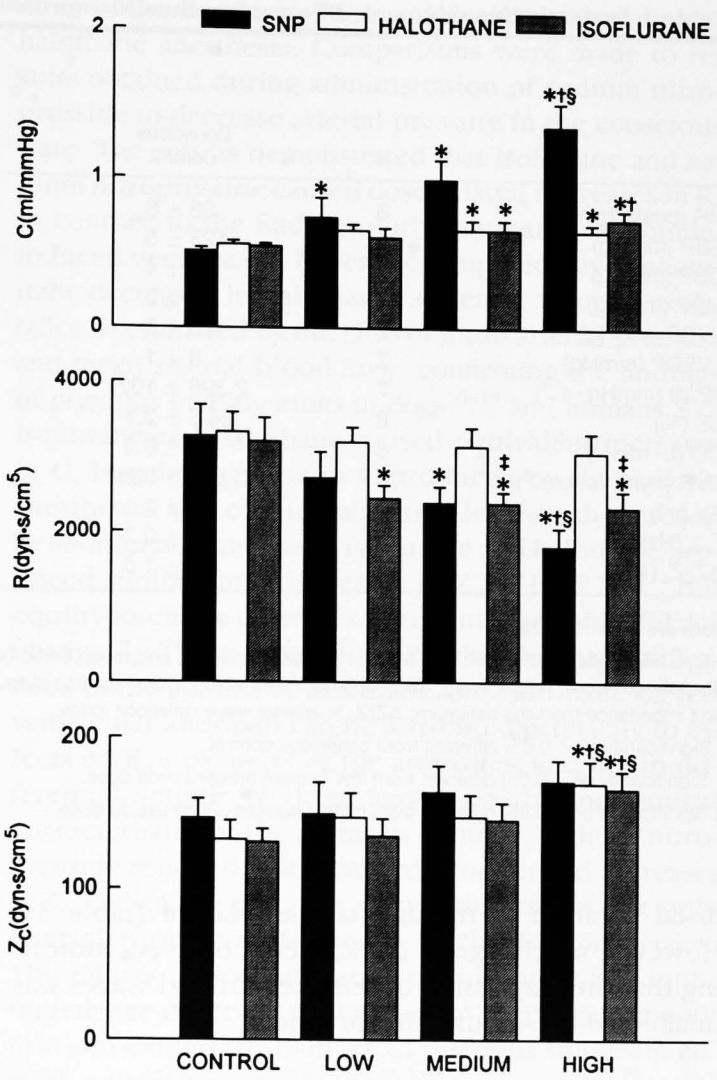

Fig. 5. Histograms depicting the effects of sodium nitroprusside (SNP), halothane, and isoflurane on total arterial compliance (C) (*top*), total arterial resistance (R) (*middle*), and characteristic aortic impedance (Z_c) (*bottom*). The low, medium, and high doses of volatile anesthetics were 1.25, 1.5, and 1.75 MAC, respectively. SNP doses were chosen to create comparable changes in mean arterial pressure (dose range 0.25–3 μg · kg^{-1} · min^{-1}). *Significantly different ($P < 0.05$) from control; †significantly different ($P < 0.05$) from the low dose; §significantly different ($P < 0.05$) from value with the medium dose; ‡significantly different ($P < 0.05$) from value with halothane at the same dose.

decreases in R (3,275 ± 417 during control to 1,812 ± 252 dyn · s · cm^{-5} during the high dose) (fig. 5). In contrast to the findings during isoflurane and halothane anesthesia, no change in Z_c was observed with the administration of sodium nitroprusside to conscious dogs. A significant decrease in F_{min} was also observed with sodium nitroprusside (3.1 ± 0.2 during control to 1.8 ± 0.2 Hz at the high dose), indicating that this drug shifts the net arterial wave reflection site to a more

Table 3. Systemic Hemodynamic Effects of Sodium Nitroprusside

	N	Conscious Control	Sodium Nitroprusside Dose		
			Low (0.25–1.0 $\mu g \cdot kg^{-1} \cdot min^{-1}$)	Middle (0.75–2.0 $\mu g \cdot kg^{-1} \cdot min^{-1}$)	High (1.5–3.0 $\mu g \cdot kg^{-1} \cdot min^{-1}$)
HR (beats/min)	8	88 ± 6	113 ± 7*	116 ± 7*	119 ± 9*
SBP (mmHg)	8	125 ± 5	103 ± 2*	83 ± 3*	74 ± 3*†
DBP (mmHg)	8	83 ± 4	75 ± 4*	55 ± 3*†	46 ± 2*†‡
MBP (mmHg)	8	95 ± 5	82 ± 4*	67 ± 3*†	51 ± 2*†
LVSP (mmHg)	7	128 ± 6	105 ± 3*	83 ± 2*	75 ± 4*†
LVEDP (mmHg)	7	8 ± 1	5 ± 0*	3 ± 0*†	3 ± 1*†
dP/dt ($mmHg \cdot s^{-1}$)	7	2,396 ± 107	2,236 ± 207	2,155 ± 140	2,243 ± 50
SS (%)	8	24.6 ± 2.1	24.6 ± 3.3	28.5 ± 2.6	28.0 ± 3.0
CO ($L \cdot min^{-1}$)	8	2.3 ± 0.2	2.0 ± 0.1	2.1 ± 0.1	2.2 ± 0.3
SVR ($dyne \cdot s \cdot cm^{-5}$)	8	3,550 ± 360	3,340 ± 300	2,680 ± 180*	2,190 ± 360*†
SV (ml)	8	26 ± 1	18 ± 1*	18 ± 1*	18 ± 1*
F_{min} (Hz)	8	3.1 ± 0.2	2.1 ± 0.1*	2.1 ± 0.1*	1.8 ± 0.2*
$\Delta Z/Z_c$ (10^2)	8	8.6 ± 1.0	7.2 ± 1.4	8.4 ± 1.7	6.2 ± 0.9

Data are mean ± SEM.

HR = heart rate; SBP, DBP, and MBP = systolic, diastolic, and mean aortic blood pressure, respectively; LVSP and LVEDP = left ventricular systolic and end-diastolic pressure, respectively; SS = segment shortening; CO = cardiac output; SV = stroke volume; SVR = systemic vascular resistance; F_{min} = frequency at first impedance modulus minimum; $\Delta Z/Z_c$ = arterial wave reflection index.

* Significantly ($P < 0.05$) different from conscious control.

† Significantly ($P < 0.05$) different from low sodium nitroprusside dose.

‡ Significantly ($P < 0.05$) different from middle sodium nitroprusside dose.

distal location in the arterial vasculature (table 3). However, no change in $\Delta Z/Z_c$ were observed, indicating that the magnitude of reflected arterial waves was unaffected by sodium nitroprusside.

Discussion

The ratio of mean arterial pressure to mean arterial blood flow (*i.e.*, systemic vascular resistance) would completely describe the hydraulic resistance of the arterial vasculature opposing cardiac ejection if the heart was a constant flow pump or if the ventricle emptied into a rigid, nondistensible tube (assuming negligible inertia of the blood). Calculated systemic vascular resistance may provide qualitative information about left ventricular afterload in the intact cardiovascular system, but systemic vascular resistance ignores the frequency-dependent characteristics of the arterial system and the viscoelastic properties of the arterial walls.[27] A simple approximation of phasic hydraulic resistance obtained by dividing instantaneous aortic pressure by instantaneous blood flow is also strictly incorrect because a frequency-dependent phase difference (time lag) between pressure and flow waves occurs as well. Aortic input impedance (Z_{in}) incorporates the viscoelastic and frequency-dependent properties of and the wave reflections that occur in the arterial vascular tree and has been shown to be a useful experimental tool for analysis of the mechanical function of the arterial system.

Z_{in} is determined by performing Fourier series or spectral analysis (using the fast Fourier transform or a periodogram technique) of aortic pressure and blood flow waveforms, transforming data from the time to frequency domain.[4,20] Z_{in} is the complex ratio of aortic pressure (the forces acting on the blood) to aortic blood flow (the resultant motion of the blood)[1,28] and is typically displayed by plotting the magnitude (modulus) and phase of Z_{in} as a function of frequency. These constitute the aortic input impedance spectrum. The $Z_{in}(\omega)$ modulus describes the ratio of the magnitude of pressure to the magnitude of flow at each point in the frequency domain. The $Z_{in}(\omega)$ phase is the difference between the phase angles of flow and pressure at each frequency. Phase angles are usually negative at low frequencies, indicating that blood flow precedes developed pressure under these conditions. Although it is clear that pathologic conditions or vasoactive drugs may alter $Z_{in}(\omega)$ by affecting the mechanical properties of the arterial wall,[8] these changes in $Z_{in}(\omega)$ are difficult

to quantify. Thus, $Z_{in}(\omega)$ is often interpreted using an analytical model known as the three-element Windkessel, an electrical analog of $Z_{in}(\omega)$ that displays most of its general characteristics in the frequency domain.[5]

The Windkessel model describes three variables that are properties of the arterial system: Z_c, R, and C. Z_c is the input impedance of the aorta minus the effects of reflected waves from the distal arterial vasculature.[1] Although it is represented as a resistor in the model for simplicity, the value of Z_c is directly related to the Poiseullian resistance of the aorta and inversely related to compliance of this vessel. Net changes in Z_c are determined by the viscoelastic properties of the aortic wall, aortic dimension, and intraaortic pressure.[1,29] R (systemic vascular resistance minus Z_c) is generally an order of magnitude greater than Z_c, consistent with the concept of the aorta as a low-resistance, high-compliance conduit and the arterioles as primary resistance vessels. Because the radius of arterial vessels varies during the cardiac cycle, R and the resistive component of Z_c can be considered mean hydraulic resistances.

The vast majority of C (>90%) is determined by aortic compliance.[30,31] The viscoelastic characteristics of the proximal aorta allow this blood vessel to store part of the energy generated by the left ventricle during ejection and return it to the arterioles and capillaries during diastole. This rectifying quality of the aorta maintains diastolic pressure and decreases arterial pulse pressure for any given mean arterial pressure. The high compliance and large diameter of the proximal aorta are responsible for the low value of Z_c in the ascending aorta, properties that contribute to decreases in wasted left ventricular power.[8] In fact, diastolic arterial pressure would decrease to zero (and coronary perfusion would cease) if the aorta and peripheral arteries were rigid tubes. Age or disease states (*e.g.*, essential hypertension or atherosclerosis) that decrease C result in lower mean diastolic pressure and increased pulse pressure. The value of C is nonlinearly related to intraarterial pressure and is determined primarily by the interrelation between collagen, elastin, and smooth muscle in the arterial wall.[8,24] Arterial distention resulting from increases in intraluminal pressure reduces C by shifting the load from the more compliant elastin fibers to the stiffer collagen fibers in the arterial wall. The Windkessel approximation of C represents a mean value for the entire arterial system because C has also been shown to vary during the cardiac cycle.[32]

In the current investigation, aortic input impedance spectra were quantified using the Windkessel parameters in the conscious state and during isoflurane and halothane anesthesia. Comparisons were made to results obtained during administration of sodium nitroprusside to decrease arterial pressure in the conscious state. The results demonstrated that isoflurane and sodium nitroprusside caused dose-related decreases in R, in contrast to the findings with halothane. Isoflurane-induced decreases in R were accompanied by concomitant decreases in calculated systemic vascular resistance as evaluated by the ratio of mean arterial pressure and mean arterial blood flow, confirming the findings of previous investigations in dogs[10–15] and humans.[16,17] Isoflurane and halothane caused equivalent increases in C, but the increase in C produced by the volatile anesthetics was considerably smaller than that caused by sodium nitroprusside. Isoflurane and halothane produced similar small increases in Z_c at 1.75 MAC, but equihypotensive doses of sodium nitroprusside did not change Z_c. These results indicate that the major difference in the actions of isoflurane and halothane on left ventricular afterload can be attributed primarily to effects on R, a property of the arterioles, and not to differential actions of these agents on the mechanical characteristics of the aorta. In contrast, sodium nitroprusside reduced R and caused pronounced increases in C, indicating that this vasodilator affects not only arteriolar tone but also aortic mechanical properties. The effects of sodium nitroprusside on aortic input impedance observed in the current investigation confirm and extend the findings of previous studies in animals and in humans.[24,28,29,33,34]

The small but significant increase in Z_c observed with isoflurane and halothane at 1.75 MAC was probably related to anesthetic-induced decreases in intraaortic pressure. Decreases in aortic diameter associated with hypotension cause increases in the Pouiseullian resistance of the aorta, leading to increases in characteristic aortic impedance. In contrast, sodium nitroprusside did not alter Z_c at an equihypotensive dose. Under these conditions, the pronounced increase in C induced by sodium nitroprusside may have balanced increases in aortic resistance. The increase in C observed during the administration of isoflurane and halothane may have also occurred as a result of hypotension because of the inverse relation between compliance and pressure (fig. 6). However, other investigations have shown that C is independent of pressure over the range of pressures observed in this investigation.[35,36] Thus, a true anesthetic-induced increase in compliance remains a possibility. The volatile anesthetics examined in the cur-

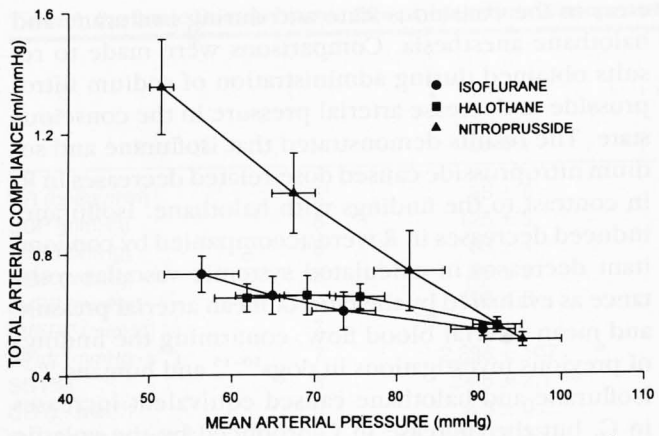

Fig. 6. Inverse relation of mean arterial pressure to total arterial compliance during control conditions (lower right corner points), sodium nitroprusside infusions (triangles), and isoflurane (circles) or halothane (squares) anesthesia for all dogs studied.

rent investigation produced very similar compliance–pressure relations; however, equihypotensive doses of sodium nitroprusside clearly increased the slope of this relation. This observation confirms the results of previous studies[26,32] and suggests that sodium nitroprusside may produce direct increases in C by affecting the mechanical compliance of the aorta, augmenting the relatively flat baseline compliance–pressure relation.[35]

The phenomenon of reflected waves in the arterial system was also evaluated using the aortic input impedance spectrum in the conscious and anesthetized states. When an arterial vessel branches, the characteristic impedance (input impedance minus the effects of wave reflection) of the proximal trunk may not be equivalent to the combined characteristic impedances of the distal branches. This hydraulic impedance mismatch causes some of the forward energy to be reflected back toward the heart. The reflected wave results in the nonisomorphic relation between arterial pressure and blood flow waveforms because the reflected wave adds to the pressure wave and subtracts from the blood flow wave. Wave reflections are manifested in aortic input impedance spectra as oscillations of $Z_{in}(\omega)$ at higher frequencies. The magnitude of the oscillations of $|Z_{in}(\omega)|$ is directly proportional to the magnitude of the wave reflections.[1] The frequency of F_{min} correlates with the distance to the major reflecting site.[1] The major reflecting site is not a true anatomic branching point but instead describes the average sum of all reflecting sites in relation to the aortic root. In the current investigation, no changes in the magnitude or net site of wave reflection were observed in the presence of isoflurane or halothane, suggesting that these volatile anesthetics have no effect on frequency-dependent, oscillatory arterial properties. In contrast, sodium nitroprusside-induced reductions in F_{min} indicate that this vasodilator shifts the net site of wave reflection to a more distal location in the arterial circulation.

The results of this investigation must be interpreted within the constraints of several potential limitations. $Z_{in}(\omega)$ was calculated using arterial pressure waveforms measured with a fluid-filled catheter system implanted in the proximal descending aorta. A high fidelity micromanometer placed at the aortic root may have provided enhanced frequency response, however, the response of the fluid-filled system was determined using a *de novo* quick release ("pop") test and the magnitude and phase of $Z_{in}(\omega)$ were appropriately corrected using established methods.[1] The distance between the pressure and blood flow transducers (approximately 4 cm) was also corrected by adjusting the magnitude and phase $Z_{in}(\omega)$.[30] The primary error introduced by spacing between the transducers occurs in the phase of $Z_{in}(\omega)$. In the current investigation, the $Z_{in}(\omega)$ phase spectra recorded in the conscious state and during sodium nitroprusside infusions were comparable to previous reports[33,37] and also agreed qualitatively with the best-fit Windkessel frequency response (fig. 3). Furthermore, none of the afterload variables derived from the Windkessel model were determined from the $Z_{in}(\omega)$ phase spectrum.

It may be observed from figure 3 that the frequency response of the Windkessel model (solid line) does not exactly match the measured aortic input impedance (open circles). The frequency response of the model (formula in fig. 1) has a magnitude equal to the sum of Z_c and R at zero frequency. The magnitude decays to Z_c at high frequencies. The rate of decay is determined by R and C. The phase of the frequency response of the model is zero at zero frequency. As frequency increases the phase reaches a minimum and then asymptotically approaches zero. The measured frequency response shows oscillations in the magnitude of the aortic input impedance spectra that are caused by reflected waves (figs. 3 and 4). The phase of the measured aortic input impedance may achieve positive phase angles because of the inertia of the blood. These aspects of the measured response cannot be accounted for by the Windkessel. The advantage of the three-ele-

ment model is its parsimony, which allows the parameters of the model to be associated with real physical parameters (*i.e.*, R, Zc, and C).[4]

Other models of the arterial system, including the transmission line (t-tube)[38–41] and other lumped parameter models,[42,43] have been proposed as alternatives to the three-element Windkessel for the quantitative interpretation of changes in left ventricular afterload assessed with $Z_{in}(\omega)$. These models may describe the fine aspects of $Z_{in}(\omega)$ in greater detail (particularly the wave reflection characteristics) but are considerably more complex to analyze and may be less physiologically intuitive than the Windkessel approach. In addition, evidence suggests that the details of $Z_{in}(\omega)$ not depicted by the three-element Windkessel model probably do not have a significant impact on its overall interpretation in terms of afterload.[4] Thus, the three-element Windkessel model used in this investigation was an appropriate choice for analysis of the effects of volatile anesthetics and sodium nitroprusside on aortic input impedance.

The $Z_{in}(\omega)$ modulus spectra obtained in anesthetized dogs were somewhat less continuous than those obtained in the conscious state (fig. 4) because some frequencies between the fundamental and corresponding harmonics were discarded on the basis of mean squared coherence criteria. This relative discontinuity in the $Z_{in}(\omega)$ modulus spectra may have introduced an error in the calculation of Z_c, $\Delta Z/Z_c$, and F_{min}. Generation of random heart rates by cardiac pacing during anesthesia would have provided a greater number of fundamental and harmonic frequencies, resulting in more continuous $Z_{in}(\omega)$ modulus spectra in the presence of isoflurane and halothane. Nevertheless, Z_c represents the arithmetic average of the $Z_{in}(\omega)$ modulus between 2 and 15 Hz, and this average was probably not significantly affected by the exclusion of some points between the fundamental and harmonic frequencies because at least six harmonics were included in each spectrum. In addition, the calculation of $\Delta Z/Z_c$ and F_{min} was probably accurate because the maximum amplitude of oscillations in $Z_{in}(\omega)$ magnitude occurred around the single fundamental and corresponding harmonic frequencies[1] in the anesthetized state, locations in the spectrum where high coherence frequencies were grouped. Lastly, the mild spectral discontinuity observed between the fundamental and harmonic frequencies during anesthesia also resembled spectra generated with standard Fourier series analysis, an established method for evaluating aortic and pulmonary input impedance and wave reflection properties under a variety of physiologic conditions.[1,8]

In summary, the results of the current investigation demonstrated that the major difference between the effects of isoflurane and halothane on left ventricular afterload quantified using the Windkessel model of $Z_{in}(\omega)$ was related to R, a property of arteriolar vessels, and not to characteristic aortic impedance or C, mechanical features of the aorta. No changes in arterial wave reflection patterns determined from $Z_{in}(\omega)$ spectra occurred with isoflurane and halothane, also suggesting that these volatile anesthetics have no effect on frequency-dependent arterial properties. In contrast, sodium nitroprusside-induced reductions in R and marked enhancement of C indicate that this vasodilator affects not only arteriolar tone but also aortic mechanical characteristics.

Appendix

The instruments used to measure aortic pressure and aortic blood flow in this investigation alter the pressure and flow waveforms used to calculate $Z_{in}(\omega)$ and must be corrected in the frequency domain to account for their frequency response. The third-order Butterworth analog low-pass filter built in to the flow meter used to assess aortic blood flow has a linear-phase response $[\theta(\omega)]$ that is a function of frequency:

$$\theta(\omega) = \arctan \cdot \{[(\omega/\omega_c{}^3 - 2(\omega/\omega_c)] \cdot [1 - 2(\omega/\omega_c)^2]^{-1}\},$$

where ω = angular frequency ($\omega = 2\pi f$) and ω_c = the cutoff frequency. The slope of this function is equal to the time delay of the flow meter. The time delay equaled 11.2 ms with the cutoff frequency set a 30 Hz. Thus, the measurement of phase of Z_{in} ($\theta_z(\omega)$) was corrected by:

$$\theta_z(\omega)^* = \theta_z(\omega) - 0.0112 \cdot \omega,$$

where $\theta_z(\omega)^*$ = the true phase of the flow signal. Because the magnitude of the frequency response of the flow meter is flat up to and beyond 15 Hz, no correction was required in the magnitude of $Z_{in}(\omega)$.

The fluid-filled catheter-pressure transducer system used to measure aortic blood pressure behaves as an underdamped second-order system governed by the differential equation:

$$M \cdot d^2x/dt^2 + B \cdot dx/dt + K \cdot x = 0,$$

where M = the mass of the system; B = the viscous damping (resistance); and K = the stiffness.[8] The frequency response of the system is determined by the damping ratio ($\xi = B \cdot [2 \cdot (K \cdot M)^{1/2}]^{-1}$) and the undamped natural frequency $[\omega_o = (K/M)^{1/2}]$. Both of these variables were derived from an input step response function obtained by performing a quick release, or "pop," test.[1,8] The catheter–pressure transducer system was subjected to a constant hydrostatic pressure that was suddenly released, allowing the measured pressure to decrease rapidly to and oscillate around 0 mmHg (fig. 7). The magnitude of the first and second oscillations around 0 mmHg (p_1 and p_2, respectively) were used to determine the logarithmic decrement (Λ):

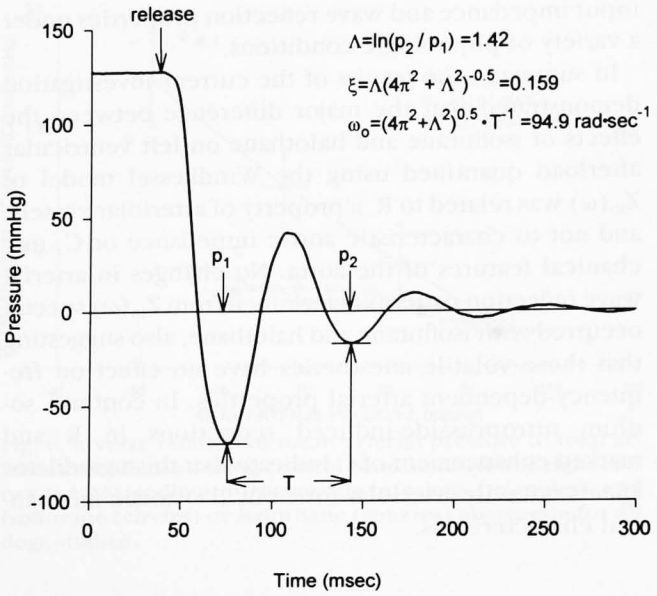

Fig. 7. Results of the quick release ("pop") test performed on the fluid-filled catheter–pressure transducer system used to measure aortic blood pressure in the current investigation. The pressure transducer was subjected to a constant hydrostatic pressure (130 mmHg) that was suddenly released, allowing the measured pressure to decrease rapidly to and oscillate around 0 mmHg. The magnitude of the first (p_1) and second (p_2) oscillations around 0 mmHg were used to calculate the logarithmic decrement (Λ). The damping ratio (ξ) and the undamped natural frequency (ω_o) were calculated, and the magnitude and phase of the aortic impedance spectrum were corrected (appendix). T = the time between p_1 and p_2.

$$\Lambda = \ln(p_2/p_1).$$

The damping ratio (ξ) was calculated from the "pop" test data using the equation:

$$\xi = \Lambda \cdot (4\pi^2 + \Lambda^2)^{-1/2}.$$

The undamped natural frequency (ω_o) was also determined empirically using the equation:

$$\omega_0 = (4\pi^2 + \Lambda^2)^{1/2} \cdot T^{-1},$$

where T = the time between p_1 and p_2. The pressure transducer system used in this investigation had a value of $\xi = 0.159$ and $\omega_o = 94.9\ \text{rad} \cdot \text{s}^{-1}$ (15.1 Hz). The magnitude of the $Z_{in}(\omega)$ spectrum was corrected (to $|Z_{in}(\omega)|$) using the expression:

$$|Z_{in}(\omega)|^* = |Z_{in}(\omega)| \cdot [(1 - \gamma^2)^2 + (2 \cdot \xi \cdot \gamma)^2]^{1/2},$$

where $|Z_{in}(\omega)|$ = the measured magnitude of $Z_{in}(\omega)$ and γ = the relative frequency (ω/ω_o).[1] The phase of $Z_{in}(\omega)$ ($\theta_z(\omega)$) was also corrected (to $\theta_z(\omega)^*$) using the formula:

$$\theta_z(\omega)^* = \theta_z(\omega) + \arctan[(2 \cdot \xi \cdot \gamma) \cdot (1 - \gamma^2)^{-1}].$$

Under ideal circumstances, $Z_{in}(\omega)$ spectra should be calculated from aortic pressure and blood flow waveforms obtained from identical locations at the aortic root. In the current investigation, aortic blood flow was measured in the ascending aorta and aortic blood pressure was measured in the proximal descending thoracic aorta just distal to the aortic arch. The difference between these measurement sites was approximately 4 cm in all dogs. Over this distance, the magnitude of the pressure signal in the frequency domain may be altered slightly, but no significant changes in the magnitude of $Z_{in}(\omega)$ would be expected.[23] An error in the phase of $Z_{in}(\omega)$ between the flow meter and the pressure transducer must be corrected, however. This phase delay ($\theta_d(\omega)$) was corrected as a function of frequency:

$$\theta d(\omega) = 180 \cdot \omega \cdot x \cdot [\pi \cdot C_{app}(\omega)]^{-1},$$

where x = the distance between measuring devices and $C_{app}(\omega)$ = the apparent wave velocity as a function of frequency. The value of $C_{app}(\omega)$ is typically quite large at low frequencies (<3 Hz) and remains fairly constant [$C_{app}(\omega) \approx 500\ \text{cm} \cdot \text{s}^{-1}$] at higher frequencies (>3 Hz).[23] Within these constraints, the phase error is negligible at low frequencies and is directly proportional to frequency at higher frequencies: $\theta_d(\omega) \approx 0.462 \cdot \omega$. Thus, the phase of $Z_{in}(\omega)$ ($\theta_z(\omega)$) was corrected (to $\theta_z(\omega)^*$) such that:

$$\theta_z(\omega)^* = \theta_z(\omega) + 0.462 \cdot \omega,$$

$\theta_z(\omega)$ phase calculations were included to insure completeness of the data, however, no Windkessel parameters were derived using $\theta_z(\omega)$ measurements.

The corrections for the frequency response of the transducers as well as the distance between transducers were generalized for all experiments. The exact frequency response of the pressure transducer will vary from day to day and from dog to dog because of microbubbles, catheter bending, or slight differences in catheter length. The exact distance between the pressure and flow transducer also will vary slightly. However, these differences would be small and impossible to measure in the conscious animal. In addition, they most likely would have little effect on the applied spectral corrections.

The authors extend their gratitude to Dr. James Ackmann, Department of Biomedical Engineering, Marquette University, for his helpful comments and suggestions. The authors also thank John Tessmer and Dave Schwabe for technical assistance and Angela Barnes for preparation of the manuscript.

References

1. Milnor WR: Hemodynamics. 3rd edition. Baltimore, Williams and Wilkins, 1989

2. Milnor WR: Arterial impedance as ventricular afterload. Circ Res 36:565–570, 1975

3. Noble MIM: Left ventricular load, arterial impedance and their interrelationship. Cardiovasc Res 13:183–198, 1979

4. Burkhoff D, Alexander JJ, Schipke J: Assessment of Windkessel as a model of aortic imput impedance. Am J Physiol 255:H742–H753, 1988

5. Elzinga G, Westerhof N: Pressure and flow generated by the left ventricle against different impedances. Circ Res 32:178–186, 1973

6. Wesseling KH, Jansen JRC, Settels JJ, Schreuder JJ: Computation of aortic flow from pressure in humans using a nonlinear, three element model. J Appl Physiol 74:2566–2573, 1993

7. O'Rourke MF: Vascular impedance in studies of arterial and cardiac function. Physiol Rev 62:570–623, 1982

8. Nichols WW, O'Rourke MF: McDonald's Blood Flow in Arteries: Theoretic, Experimental, and Clinical Principles. 3rd edition. Philadelphia, Lea & Febiger, 1990, p 456

9. Sagawa K, Maughan L, Suga H, Sunagawa K: Cardiac Contraction and the Pressure-volume Relationship. New York, Oxford University Press, 1988, p 480

10. Merin RG, Kumazawa T, Luka NL: Myocardial function and metabolism in the conscious dog and during halothane anesthesia. ANESTHESIOLOGY 44:402–415, 1976

11. Merin RG: Are the myocardial functional and metabolic effects of isoflurane really different from those of halothane and enflurane? ANESTHESIOLOGY 55:398–408, 1981

12. Merin RG, Bernard JM, Doursout MF, Cohen M, Chelly JE: Comparison of the effects of isoflurane and desflurane on cardiovascular dynamics and regional blood flow in the chronically instrumented dog. ANESTHESIOLOGY 74:568–574, 1991

13. Pagel PS, Kampine JP, Schmeling WT, Warltier DC: Comparison of the systemic and coronary hemodynamic actions of desflurane, isoflurane, halothane, and enflurane in the chronically instrumented dog. ANESTHESIOLOGY 74:539–551, 1991

14. Horan BF, Prys-Roberts C, Roberts JG, Bennett MJ, Foex P: Haemodynamic responses to isoflurane anaesthesia and hypovolaemia in the dog, and their modification by propranolol. Br J Anaesth 49: 1179–1187, 1977

15. Prys-Roberts C, Gersh BJ, Baker AB, Reuben SR: The effects of halothane on the interactions between myocardial contractility, aortic impedance, and left ventricular performance: I. Theoretical considerations and results. Br J Anaesth 44:634–649, 1972

16. Eger EI II, Smith NT, Stoelting RK, Cullen DJ, Kadis LB, Whitcher CE: Cardiovascular effects of halothane in man. ANESTHESIOLOGY 32:396–409, 1970

17. Stevens WC, Cromwell TH, Halsey MJ, Eger EI II, Shakespeare TF, Bahlman SH: The cardiovascular effects of a new inhalation anesthetic, Forane, in human volunteers at constant arterial carbon dioxide tension. ANESTHESIOLOGY 35:8–16, 1971

18. Pagel PS, Kampine JP, Schmeling WT, Warltier DC: Comparison of end-systolic pressure–length relations and preload recruitable stroke work as indices of myocardial contractility in the conscious and anesthetized, chronically instrumented dog. ANESTHESIOLOGY 73: 278–290, 1990

19. Theroux P, Franklin D, Ross J Jr, Kemper WS: Regional myocardial function during acute coronary artery occlusion and its modification by pharmacologic agents in the dog. Circ Res 35:896–908, 1974

20. Taylor MG: Use of random excitation and spectral analysis in the study of frequency-dependent parameters of the cardiovascular system. Circ Res 18:585–595, 1966

21. Challis RE, Kitney RI: Biomedical signal processing (in four parts): III. The power spectrum and coherence function. Med Biol Eng Comput 29:225–241, 1991

22. Marple SL Jr: Digital Spectral Analysis: With Applications. Englewood Cliffs, Prentice-Hall, 1987

23. Westerhof N, Noordergraaf A: Errors in the measurement of hydraulic input impedance. J Biomech 3:351–356, 1970

24. Pepine CJ, Nichols WW, Curry RC Jr, Conti CR: Aortic input impedance during nitroprusside infusion: A reconsideration of afterload reduction and beneficial action. J Clin Invest 64:643–654, 1979

25. Murgo JP, Westerhof N, Giolma JP, Altobelli SA: Aortic input impedance in normal man: Relationship to pressure wave forms. Circulation 62:105–116, 1980

26. Liu Z, Brin KP, Yin FCP: Estimation of total arterial compliance: An improved method and evaluation of current methods. Am J Physiol 251:H588–H600, 1986

27. Fung YC: Biomechanics: Mechanical Properties of Living Tissues. 2nd edition. New York, Springer-Verlag 1993, p 568

28. O'Rourke MF, Taylor MG: Input impedance of the systemic circulation. Circ Res 20:365–380, 1967

29. Yin LCP: Aging and vascular impedance, Ventricular/Vascular Coupling. Edited by Yin LCP. New York, Springer-Verlag, 1987, p 406

30. Westerhof N, Bosman F, De Vries CJ, Noordergraaf A: Analog studies of the human systemic arterial tree. J Biomech 2:121–143, 1969

31. Ferguson JJ III, Miller MJ, Sahagian P, Aroesty JM, McKay RG: Assessment of aortic pressure-volume relationships with an impedance catheter. Cathet Cardiovasc Diagn 15:27–36, 1988

32. Li JKJ, Cui T, Drzewiecki GM: A nonlinear model of the arterial system incorporating a pressure-dependent compliance. IEEE Trans Biomed Eng 37:673–678, 1990

33. Gundel W, Cherry G, Rajagopalan B, Tan LB, Lee G, Schultz D: Aortic input impedance in man: Acute response to vasodilator drugs. Circulation 63:1305–1314, 1981

34. Little WC, Cheng CP: Left ventricular-arterial coupling in conscious dogs. Am J Physiol 261:H70–H76, 1991

35. Van Den Bos GC, Westerhof N, Elzinga G, Sipkema P: Reflection in the systemic arterial system: Effects of aortic and carotid occlusion. Cardiovasc Res 10:565–573, 1976

36. Alexander J Jr, Burkhoff D, Schipke J, Sagawa K: Influence of mean pressure on aortic impedance and reflections in the systemic arterial system. Am J Physiol 257:H969–H978, 1989

37. Kelly RP, Ting CT, Yang TM, Liu CP, Maughan WL, Chang MS, Kass DA: Effective arterial elastance as index of arterial vascular load in humans. Circulation 86:513–521, 1992

38. Campbell KB, Burattini R, Bell DL, Kirkpatrick RD, Knowlen GG: Time-domain formulation of asymmetric T-tube model of arterial system. Am J Physiol 258:H1761–H1774, 1990

39. Burattini R, Campbell KB: Modified asymmetric T-tube model to infer arterial wave reflection at the aortic root. IEEE Trans Biomed Eng 36:805–814, 1989

40. Burattini R, Knowlen GG, Campbell KB: Two arterial effective reflecting sites may appear as one to the heart. Circ Res 68:85–99, 1991

41. Burattini R, Campbell KB: Effective distributed compliance of the canine descending aorta estimated by modified T-tube model. Am J Physiol 264:H1977–H1987, 1993

42. Burattini R, Fogliardi R, Campbell KB: Lumped model of terminal aortic impedance in the dog. Ann Biomed Eng 22:381–391, 1994

43. Grant BJB, Paradowski LJ: Characterization of pulmonary arterial input impedance with lumped parameter models. Am J Physiol 252:H585–H593, 1987